

Characterization of Engineered Biochar: Proximate Analyses, Ultimate Analyses, Physicochemical Analyses, Surface Analyses, and Molecular Analyses



Kacper Świechowski, Waheed Adewale Rasaq, Sylwia Stegenta-Dąbrowska, and Andrzej Białowiec

Abstract In recent times, biochar production, its modification, and utilization have gained much attention. The uniqueness of biochar properties allows its ease in modification to meet up with the application requirements. Low production cost, abundance of raw material, and its applications have contributed to enhancing the research work of biochar. Various biochar production pathways (raw material, process conditions) and their utilization require standardization to maintain quality. In this chapter, the characterization of engineered biochar is explained in detail, which provides robust insight into the analyses, procedures, and expected results for a typical biochar. Specifically, proximate, ultimate, physicochemical, surface, and molecular analyses are described.

Keywords Biochar · Pyrolysis · Thermal conversion

1 Introduction

The area of biochar production, utilization, and engineering is attracting attention due to its applicability in many different fields, low-cost production, environmental-friendly impact, and its use as a tool that can help solve global problems related to climate change, environmental pollution, and soil degradation (Mayer et al. 2014). Different applications, for example, solid fuel productions, pollutants removal, carbon sequestration, soil amelioration (Oliveira et al. 2017), odors mitigation from

K. Świechowski (✉) · W. A. Rasaq · S. Stegenta-Dąbrowska · A. Białowiec
Department of Applied Bioeconomy, Wrocław University of Environmental and Life Sciences,
37/41 Chełmońskiego Str., 51-630 Wrocław, Poland
e-mail: kacper.swiechowski@upwr.edu.pl

W. A. Rasaq
e-mail: waheed.rasaq@upwr.edu.pl

S. Stegenta-Dąbrowska
e-mail: sylwia.stegenta-dabrowska@upwr.edu.pl

A. Białowiec
e-mail: andrzej.bialowiec@upwr.edu.pl

livestock production (Chen et al. 2021a; Lee et al. 2021), biological processes of organic waste treatment (methane fermentation and composting) (Malinowski et al. 2019), supercapacitor and high yield sorbent material production (Bartoli et al. 2020), geoenvironmental engineering (Wani et al. 2021) require biochar with completely different properties.

Different analyses have been either developed or adopted from other fields to analyze and compare biochar. In this chapter, standard methods and results to be expected are described. The methods are ordered from the most used like proximate analysis to more sophisticated molecular analyses. Analyses and biochar properties described in this work are presented in Fig. 1. The presented classification is simplified, because some methods/properties may belong to more than one group of analyses. The analyses are divided into five subsections, namely: proximate, ultimate, physicochemical, surface, and molecular analyses. The chapter ends with the main conclusions and future prospects of biochar analyses.

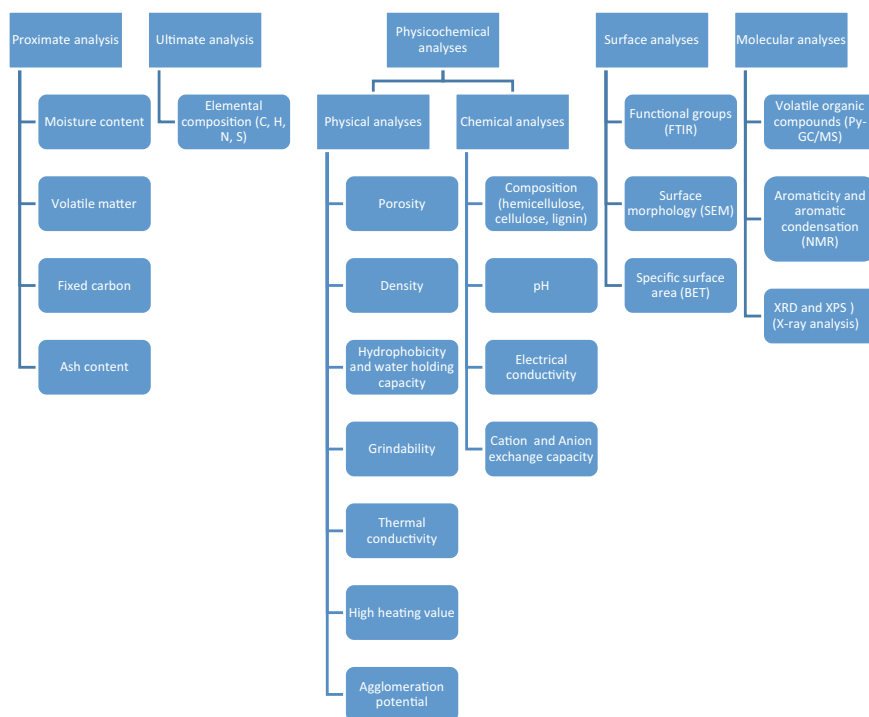


Fig. 1 Analyses classification covered in present chapter

2 Proximate Analysis

The proximate analysis has been used for over 180 years (Suárez-Ruiz and Ward 2008). It is one of the most basic, and widespread analyses used mainly for solid fuels comparison. The data from the analysis provides information about moisture content (MC), volatile matter (VM), fixed carbon (FC), and ash (AC) in fuel. These properties are related to the amount of water, materials that burn in either gaseous and solid state, and the mass of inorganic residues contained in the fuel, respectively (Nunes et al. 2018). There are many standards for proximate analysis such as ISO (International Organization for Standardization), ASTM (American Society for Testing and Materials), and a lot of variations for materials, e.g., ASTM D3172-13 for coals, or ISO 18122 and ISO 18123 for biofuels. Though proximate analysis is a relatively simple analysis, some methods were developed to perform it quicker, for example, by using thermogravimetric equipment (Torquato et al. 2017). As biochar is made from biomass and its properties resemble coal properties, using the aforementioned standards or methods appears fitting.

Regardless of the standard used, the proximate analysis is about the heating of analyzed material in specific conditions (temperatures, times, and atmospheres). Different standards varied mainly by slight differences in temperature, time, and device used. First, a raw sample is dried at 105 °C until the mass losses resulting from water evaporation stops. During drying some volatile organic compounds may also be released. Then the difference in mass before and after drying moisture content is calculated. The dry sample is then pyrolyzed at 950 °C for 7 min. The difference in mass before and after pyrolysis is the mass of volatile matter. Then, the sample is burned at 600–700 °C, and the residue that result is ash. After that, the fixed carbon is calculated by subtraction from 100%, the sum of the percentage share of moisture content, volatile matter, and ash content.

The results of the proximate analysis can be given in four ways. The air-dry sample is related to mass after surface water is removed. Additionally, the dry basis presents the result that is related to the mass of the sample after all possible removal of moisture (by drying at 105 °C). A dry ash-free (daf) basis presents results that are related to the mass of the sample after all moisture and ash have been removed (Torquato et al. 2017).

The properties of proximate analysis differ significantly between biochar, and the main reason for this is the variation in pyrolysis conditions and raw materials. The temperature typically varies from 200 to 800 °C, from several minutes up to hours. Biochar can be made from any organic materials like wood, or non-wood raw material, e.g., agricultural waste (plants, manures), sewage sludge, algae, etc. (Jafri et al. 2018). In general, higher temperatures and longer residence times promote an increase in fixed carbon and ash content in biochar. It follows from the fact that during pyrolysis all moisture content is removed and most volatiles are released. The more severe the process conditions, the more volatiles are released. Moreover, some volatiles can be converted into fixed-carbon if they stay too long in the reactor due to secondary reactions (Safdari et al. 2018). As a result, depending on the used

raw material, ash content differs from 1 to 20%, wherein it is higher for non-wood biochar than wood-based biochar. The content of volatile matter in biochar differs from 6 to 88%, whereas fixed carbon differs from 11 to 86% (Jafri et al. 2018).

Based on the proximate analysis results, the fuel ratio (FR) can be calculated. FR is the ratio of fixed carbon to volatile matter. The FR for different coals is ≥ 10 for anthracite, 6–10 for semi-anthracite, 3–6 for semi-bituminous, and < 3 for bituminous (Thrush 1968). In comparison wood and wood-based biochar made at 220, 350, and 550 °C in 30 min, have an FR value of 0.13, 0.16, 1.23, and 5.6, respectively (Wang and Howard 2018). Kim et al. (2019) have established a correlation between FR and the emission of NO_x for coal. Their work showed the possibility of predicting NO_x emission during biochar/coal combustion (Kim et al. 2019).

The additional useful biochar properties are total solids (dry mass) and the volatile solids (VS) content (loss of ignition or organic matter content). Both TS and VS are not a part of the proximate analysis but their determination is done by a similar method. The TS can be determined by subtraction from 100% of the moisture content. The VS is determined after dry sample incineration at 550 °C, where the difference between initial mass and residues is a mass of VS. The % share of VS is always related to the dry mass of the sample (Kelly Orhorhoro et al. 2017). These parameters are important for biochar used as an additive for biological processes like methane fermentation/ composting (Kelly Orhorhoro et al. 2017; Stegenta-Dąbrowska et al. 2020).

3 Ultimate Analysis

The ultimate analysis (elemental analysis) is the term given for the determination of carbon (C), hydrogen (H), nitrogen (N), sulfur (S), and oxygen (O) content in the sample. The C, H, N, S, and O elements are the main constituents of solid biofuel (Caillat and Vakkilainen 2013). Besides the different analyzers, there are equally varied approaches to determining the elemental composition, but the basic principles remain the same. The sample is combusted at 1000 °C by using pure oxygen. As a result, the elements C, H, N, and S are converted into carbon dioxide, water, oxides of nitrogen, and sulfur dioxide, respectively (Ramola et al. 2014). Next, combustion products are carried by using helium gas heated at around 600 °C in a copper tube. The copper removes all residual oxygen and converts any nitrogen oxides into nitrogen gas. Then, combustion gases are carried further through the absorbent traps in order to remove unwanted gases, e.g., hydrogen chloride. Finally, the clean carbon dioxide, water, nitrogen, and sulfur dioxide can be quantified by using gas chromatography, or by separate infrared and thermal conductivity cells (Thompson 2008).

From an energetic point of view, biochar with high carbon content is desired. C, H, and S are elements that contribute to increasing the heating value. Nevertheless, during pyrolysis, most of the H will go to the volatile matter, and S will be the source of unwanted SO_x emissions. Also, N contained in the fuel is the main source of NO_x emission (Caillat and Vakkilainen 2013). The concentration of elements in

biochar varies significantly depending on substrate and pyrolysis regime. In previous work, 10 substrates were pyrolyzed from 300 up to 500 °C and residence times of 20–60 min (with intervals of 20 °C and 20 min) (Świechowski et al. 2020). The results showed that for some materials, the pyrolysis process results in increasing the carbon content with an increase in temperature. Materials that followed this trend were fabrics, and wood, where C content increased from 44 and 47% up to 71 and 67%, respectively, for biochar made at 500 °C. Other materials like kitchen waste or paper were characterized by an initial increase in the carbon content at lower temperatures in comparison with the raw material, but with increasing temperature, the C content decreased. Moreover, for materials like plastic, rubber, or refuse solid fuel, the C content decreased compared to raw material at all temperatures (Świechowski et al. 2020, 2021). Regardless of processed material, the devolatilization results in hydrogen and oxygen removal. The mass of removed H and O depends mainly on the temperature and it increases with an increase in temperature. As result, biochar has lower H and O content in comparison with raw materials used for their production (Ramola et al. 2014; Świechowski et al. 2020, 2021). Since each of the elements is removed at a different rate depending on process conditions, the final elemental composition is the result of the weight loss of the individual components and ash residues (Zhang et al. 2018).

Besides, the elemental composition is used to perform graphical solid fuel classification. It is done by plotting a modified Van Krevelen diagram that shows the degree of coalification and energy densification (Pudasainee et al. 2020). The diagram has two axes, on the y-axis is the atomic H to C ratio, whereas on the x-axis is the atomic O to C ratio (Pudasainee et al. 2020). The atomic ratios can be calculated by using the following equations; $H/C = (H/1)/(C/12)$, $O/C = (O/16)/(C/12)$, where the numbers stand for the atomic masses of elements (Świechowski et al. 2019). Commonly, the diagram is ordered into 5 groups; anthracite, coal, lignite, peat, and biomass. The value of the H/C ratio varied from 0.1 for anthracite to 2 for biomass, and the value of the O/C ratio varied from 0.1 to 1 for anthracite and biomass, respectively. Generally, the lower the O/C and H/C ratios, the greater the energy and the higher coalification (Pudasainee et al. 2020). By plotting the biochar elemental composition on the modified Van Krevelen diagram, biochar classification and end uses determination are possible. Depending on the raw material and pyrolysis conditions, biochar H/C ratio values vary from 0.4 to 1.2, and the O/C ratio varies from 0.2 to 0.4 (Santín et al. 2017). Additionally, the knowledge of the elemental composition of biochar allows the indirect calculation of the higher heating value of biochar. For example, a modification of Dulong's formula can be used (Hosokai et al. 2016).

$$HHV = 33.8C + 1.223 \left(H - \left(\frac{O}{8} \right) \right) + 9.4S \quad (1)$$

where

HHV —high heating value of fuel, MJ kg^{-1} ,

C —elemental carbon content in dry fuel, %

- H*—elemental hydrogen content in dry fuel, %
O—elemental oxygen content in dry fuel, % and
S—elemental sulfur content in dry fuel, %.

Besides the ultimate analysis, other elements are also determined for biochar. When used for energy purposes (e.g., co-fired in boiler), the knowledge about oxides is useful for the calculation of slagging and fouling indicators. There are many different indicators and most of them are based on SiO₂, CaO, K₂O, P₂O₅, Fe₂O₃, Al₂O₃, MgO, Na₂O, and SO₃ composition (Lachman et al. 2021). When biochar is used as an additive for biological processes or a soil amendment, other elements need to be determined. These include macronutrients (P and S) and micronutrients (Ca, K, Mg, Na, Fe, Mn, Zn) (Morales et al. 2015). These macro- and microelements are determined by using inductively coupled plasma optical emission spectrometry (ICP-OES) according to ISO 11885:2009 standard. Morales et al. (2015) analyzed micro and macro elements in 102 different biochar. The amount of P, S, Ca, K, Mg, Na, Fe, and Zn varied significantly depending on pyrolyzed substrate and process conditions. An increase in temperature slightly increased the P content for manure and kitchen waste-derived biochar, while a slight decrease was observed for wood biochar. For other materials the changes were imperceptible. For most of the tested biochar, the increasing temperature had no significant effect on Ca and S content. In general, the value of Ca slightly increased or remained unchanged. The highest increase in Ca was observed for biochar made of paper and chicken manure. An increase in process temperature led to an increase in the amount of K, Mg, and Mn in the biochar. For some materials, the increase was insignificant, while for materials such as manure, corn, and kitchen waste the increase was significant. Regardless of the raw materials, pyrolysis resulted in a slight increase in Fe content, especially for materials like cattle manure waste, food waste, and paper waste (Morales et al. 2015).

4 Physicochemical Analyses

4.1 Physical Analyses

4.1.1 Porosity

In pyrolysis when temperature increases beyond 500 °C, the degree of porosity differs in different raw materials. It was investigated that biochar produced at 350 °C resulted in an average porosity $\leq 10 \mu\text{m}$ (Weber and Quicker 2018; Batista et al. 2018).

Porosity is described as the percent of the biochar particle volume not filled by solid (Brewer et al. 2014). This would include all pore volumes that open directly to the exterior of the biochar particle, yet are smaller than the DryFlo[®] particle standard size of 75–8000 μm (Wade et al. 2015). According to Plötze and Niemz (2011) porosity of biochar can be calculated as follows:

$$n = 1 - \rho / \rho_s \times 100 \quad (2)$$

where

- n—porosity in percent,
- ρ —oven-dry bulk density, and
- ρ_s —specific solid density.

Some parameters have been associated with porosity, like pore accessibility and mercury porosimetry. Pore accessibility is when pores within given particles would not all have access to the exterior (Brewer et al. 2014). Mercury porosimetry can be used to determine the pore size distribution and porosity of biochar. It is used by applying pressure to a sample immersed in mercury. The applied external pressure for mercury penetrates the biochar pores, because of the high contact angle of mercury. The specific amount of pressure required to intrude into the pores is inversely proportional to sample pores size. The larger the pore, the smaller the pressure needed to penetrate the pores (Anderson 2021). This can be determined, for example, using Auto Pore IV mercury porosimeter (Micromeritics, Norcross, GA) (Brewer et al. 2014).

4.1.2 Density

The density simply refers to a measure of mass per unit volume. The density of wood biochar is a very vital parameter especially after it undergoes the pyrolysis process. Just like how hardwood is different from softwood, different types of wood raw material would vary across biochar density with pyrolysis temperature (Plötze and Niemz 2011; Brewer et al. 2014; Weber and Quicker 2018). Some parameters have been associated with density. These include envelope density, skeletal density, and true density/true particle density. The envelope density is the ratio of the sample mass of biochar particles to the sum of the volume of wood biochar sample in each piece and the voids within each piece. This means that within close-fitting imaginary envelopes surrounding each piece and it takes the solid structure, all pores, and surface irregularities into consideration (Webb 2001). Envelope density typically is determined by (ASTMD3766), using, for example, Geopyc 1360 Envelope Density Analyzer (Micromeritics, Norcross, GA). The ratio of wood biochar particle mass can also be measured by the BSI standard (Webb 2001; Brewer et al. 2014). The bulk density of wood biochar refers to the total mass of solid material divided by the volume occupied, which include the space between the biochar particle (Webb 2001). As gases devolatilize from the wood biomass structure during pyrolysis, a porous char remains behind. Higher porosity means lighter char per unit volume (Plötze and Niemz 2011). Bulk density can be measured by (ASTMD5004). The skeletal density involves two facets namely: (a) the mass of the discrete pieces of solid material; and (b) the sum of the volume of solid material in the pieces and closed pores within the pieces. Understanding the skeletal density requires the ratio between these above-mentioned two facets, and it can be determined by ASTMD3766 (Webb

2001; Brewer et al. 2014). The true density/true particle density of biochar particle is the mass of a wood material after it has undergone the pyrolysis process, divided by its volume without including open and closed pores (Webb 2001).

4.1.3 Micropore Volume

Micropore, mesopore, and macropore volume, respectively, are categorized by pore sizes $<2 \mu\text{m}$, $<50 \mu\text{m}$, and $>50 \mu\text{m}$, all of which occur in biochar (Paar). Micropore volume is influenced by the pyrolysis temperature. The type of raw material also influences the total pore volume. Biochar formed at 400, 600, and 800 °C with a micropore volume range (5–30 μm) of biochar produced from woody biomass are larger than those formed by another raw material (Kameyama et al. 2019). Micropore volume can be measured by using an Autosorb-3b gas sorption analyzer (Quantachrome Instruments, Boynton Beach, FL) (Brewer et al. 2014).

4.1.4 Hydrophobicity and Water-Holding Capacity

The decrease in functional groups alters the affinity of biochar toward the water and an increase in porosity changes the amount of water that can be adsorbed (Brewer et al. 2014). Depending on the pyrolysis temperature, samples produced at 400 °C would appear to have higher hydrophobic properties than that biochar samples formed at a temperature range of 600–800 °C. This simply reflects that low pyrolysis temperature might increase the hydrophobicity of biochar, resulting in limiting the water retention capacity (Kameyama et al. 2019; Masís-Meléndez et al. 2020). Hydrophobicity and water-holding capacity of biochar can be measured by using the mercury intrusion porosimetry (MIP) method, plant-available water capacity (AWC), and water-retention curve (WRC). According to some workers (Kinney et al. 2012), the surface hydrophobicity of biochar samples can be determined by using the molarity of an ethanol drop (MED) test.

4.1.5 Grindability

Grindability refers to the ability of a (wood) biomass material to be made smaller by grinding. Typically, grindability explains the characteristic of coal particularly the ease by which it pulverizes. It can also be considered as mechanical properties of given biochar that could limit its overall applicability (Weber and Quicker 2018). However, the pyrolysis or torrefaction usually reduces the energy required for grinding biomass material and the process temperature is the most important parameter that influences grindability, as the grindability index of the processed biomass increases with the temperature (Repellin et al. 2010; Basu 2018). The standard method of biochar grindability analysis is Hardgrove Grindability Index (HGI). It was investigated by numerous studies that the lower HGI measure depicts that the

biomass material is poorly grindable and the higher measure value indicates that the material is grindable (Weber and Quicker 2018).

The HGI measuring method involves the use of a miniature ball mill type of pulverizer that comprises ground coal of standard mass size (50 g) within a specific time and known force. The resultant product, when subject to a sieve of standard mesh size (75 μm), would be compared with the amount of the material sieve size of the desirable/specified reference standard (Basu 2018). The grindability index of biomass samples is influenced by the pyrolysis temperature and it also depends on the biomass type. For example, poplar wood investigated by Basu (2018) showed that process temperatures of 210 and 270 $^{\circ}\text{C}$ resulted in 8 and 47 HGI, respectively.

4.1.6 Thermal Conductivity

The thermal properties and yields of biochar depend on raw material, pyrolysis temperature, and the direction of heat flow (Yang et al. 2017; Weber and Quicker 2018). Moreover, the higher density of biomass material typically leads to a higher conductivity value and porous structure results in decreased thermal conductivity of biochar compared to the raw material (Weber and Quicker 2018). The direction of the heat flow impacts the value of thermal conductivity (Weber and Quicker 2018) as the highest value is obtained when the heat flow is parallel to the biomass sample direction at a range of 1.5–2.7 times in comparison to the perpendicular direction. Thermal conductivity and heat flow in the context of biochar can be measured by using NETZSCH HFM 446 Heat Flow Meter following ASTM C518 (Jeon et al. 2021).

4.1.7 The High Heating Value (HHV)

The HHV of biochar produced from raw material is one of the important parameters in the consideration of energy analyses, which can be defined as the energy released per unit mass (Yang et al. 2017). The HHV of biomass material depends and varies with pyrolysis temperature and raw material. (Yang et al. 2017) analyzed biochar produced from eight different biomass types that undergo pyrolysis process in two selected temperature values (350 and 500 $^{\circ}\text{C}$). HHVs of pyrolyzed biochar produced from Miscanthus and bamboo sawdust at 500 $^{\circ}\text{C}$ were higher than samples formed at 350 $^{\circ}\text{C}$, while the opposite result was obtained in the case of rice straw and bamboo leaves biochar. However, most of these examined raw materials had similar HHVs values (ranging from 18.44 to 20.10 MJ kg^{-1}) except pecan shells and rice straw which appeared lower at 15.85 and 16.95 MJ kg^{-1} , respectively. HHV can be measured using bomb calorimeter ASTM 200. Briefly, this would involve a given amount of sample (1 g) placed into the bomb chamber that is linked to the ignition wire by a specific thread. This would follow by the vessel being filled with oxygen at a pressure of up to 30 bar. After the ignition, the core temperature of the crucible

can increase to 1,000 °C during the combustion of organic material. Finally, the heat value can be determined (Basu 2018).

4.1.8 Agglomeration Potential

Agglomeration of pyrolyzed biochar is typically a way to increase the strength and density of biochar, to make it easier to transport for economical benefit, preservation, and suitable handling (Weber and Quicker 2018). The agglomeration potential in the context of biochar can be performed in two common ways such as press agglomeration, which can be achieved by applying pressure and tumble agglomeration method, which can be done by the tumbling process. Weber and Quicker 2018 stated that agglomeration potential is slightly influenced by process temperature, in the sense that at <200 °C, it is higher while seems to be stable at temperature >200 °C. Basu 2018 showed the impact of raw materials such as straw, sunflower husk, wood chips, sawdust, and rice husk on agglomeration potential values (5, 4, 1, 1, and 0) respectively.

4.2 Chemical Analyses

4.2.1 Composition (Hemicellulose, Cellulose, and Lignin)

Wood and agricultural waste-derived biochar are made up of hemicellulose, cellulose, and lignin constituents. As a result, the concentration of these constituents does impact the pyrolysis process and the physical properties of biochar. For example, biochar produced from animal litter has lower carbon content, specific surface area, and higher cation exchange capacity than biochar produced from wood. The reason for this is the difference in lignin and cellulose content (Tomczyk et al. 2020). During pyrolysis, hemicellulose and cellulose are mainly responsible for volatile matter production, whereas lignin is responsible for solid products (Narzari et al. 2015). Hemicellulose is a complex mixture of polysaccharides, and most of them almost completely decompose at 200–380 °C (Werner et al. 2014). Cellulose is more temperature resistant and its degradation takes place at 300–350 °C. Lignin is the most thermal resistant and decomposes at 300–500 °C (Carrier et al. 2011). There are two main ways to determine the composition of these constituents. According to wood industry methodology, tested material is pre-treated at the beginning to remove extractives. Then lignin, holocellulose, and α -cellulose extraction are done. According to food industry methodology, tested materials are pre-treated for neutral detergent fiber (NDF) determination. Then, acid detergent fiber (ADF), and acid detergent lignin (ADL) are determined. Both methods with procedures are described in the work of (Carrier et al. 2011).

4.2.2 pH Analysis and Electrical Conductivity (EC)

The pH value of biochar is an important property for agricultural applications such as soil amendment (Weber and Quicker 2018). Biochar pH value and electrical conductivity (EC) are measured with a glass electrode connected to a digital pH meter. Biochar is a dry material, and pH and EC can be obtained from a sample mixed with deionized water or KCl. Samples are generally stirred thoroughly and allowed to stand for a different time before measurement (Fig. 2). Different biochar-to-water or biochar -to - KCl ratios, are (i) biochar-to-water/KCl ratio of 1:10 (Al-Wabel et al. 2013), (ii) biochar-to-water/KCl ratio of 1:20 solution, after 12 h rest and stirring of suspension (Rodriguez et al. 2021), (iii) 1 g of sample with 60 ml distilled water, the solution was then shaken for 1 h in a shaker and allowed to cool to room temperature (Bian et al. 2018).

Zhao et al. (2021) showed that, under different pyrolysis temperatures, the electrical conductivity varied in the biochar. EC of biochar increased with the increment of temperature. For example, EC of biochar at 400, 600, 800, and 1000 °C was 0.001, 0.03, 0.8, and 6.3 S m⁻¹, respectively. Additionally, the EC increased drastically when the temperature exceeded 800 °C (Zhao et al. 2021). The electrical conductivity of biochar positively depends on the degree of carbonization.

Interestingly a new phenomenon has been termed, i.e., “elastic behavior of electrical conductivity of biochar” meaning EC increased with compressive loading and dropped to the pre-compression level when the loading is released (Gabhi et al. 2017). In general, biochar generated from various organic waste is characterized by lower electrical conductivity compared with other carbon materials (Shao et al. 2019). Higher pyrolysis temperature increases the pH of most biochar. Ahmad et al. (2012)

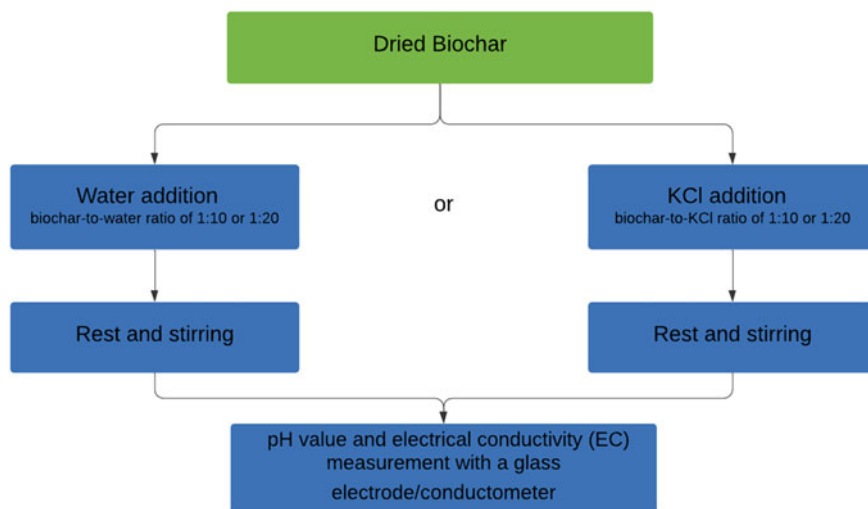


Fig. 2 Scheme of pH analysis and electrical conductivity (EC) measurement in biochar

discovered that pH value is a direct result of an increasing degree of carbonization. Increasing pyrolysis temperature generally increases the pH of biochar by producing more alkaline components, ash contents, and exchangeable and soluble cations (Li and Chen 2018).

4.2.3 Cation Exchange Capacity and Anion Exchange Capacity

The cation-exchanging ability or lack thereof of biochar is evident by the magnitude of its cation exchange capacity (CEC) (Das et al. 2010). The CEC is defined as the number of exchangeable cations (e.g., K^+ , Na^+ , NH_4^+ , Mg^{2+} , Ca^{2+} , Fe^{3+} , Al^{3+} , Ni^{2+} , and Zn^{2+}), often expressed as centimoles (cmol) or millimoles (mmol) of total or specific cations per kilogram (kg) of soil. <50 mmol kg^{-1} of CEC in the soil is regarded as serious deficiency, >50 and ≤ 250 mmol kg^{-1} is a moderate CEC range, and >250 mmol kg^{-1} is exceptionally high CEC Lee et al. (2013).

CEC measurement is performed in modified protocol from AOAC method 973.09 (Rippy and Nelson 2007). The procedure for CEC analysis is given elsewhere (Huff et al. 2018).

(Rizwan et al. 2016) reported that the higher cation exchange capacity of the biochar means higher adsorption of metals. However, the cation exchange capacity decreased with pyrolysis temperatures >350 °C.

CEC content in biochar gives important information for biochar usefulness as a possible adsorbent of different pollutants. The exchange of protons and ionized cations with dissolved salts on the biochar surface is the main principle of the CEC mechanism. Biochar adsorption capacity to remove heavy metals depends upon the pollutant size and surface functional group of the biochar (Rizwan et al. 2016). For example, (Trakal et al. 2016) investigated the removal of Cd and Pb using biochar prepared from different raw materials such as wheat straw, grape stalk, grape husk, plum stone, and nutshell. The results showed higher Pb and Cd removal efficiency for the raw material containing iron oxides. The presence of iron in the raw material enhanced the cation exchange capacity of the biochar (Ambaye et al. 2021).

It is known that biochar which has an increased CEC generally possesses a greater nutrient retention capacity. These biochars with greater CEC generally possess a significant amount of hydrophilic oxygen-containing groups, such as phenolic and carboxylic groups, which impart the greater cation exchangeability (Das et al. 2010). The mechanisms responsible for the change of CEC in biochar are well established. However, the evidence presented by Cheng et al. (2008) indicates that biochar AEC pathways are not fully understood. Furthermore, biochar with high AEC has the potential to be used in water treatment for the removal of anionic contaminants; hence high AEC is a potentially useful property that may contribute to biochar value. Biochar AEC is limited under neutral and alkaline conditions (Lawrinenko and Laird 2015).

AEC is measured by Cl^- for Br^- compulsive exchange of 1 g biochar samples in water for which Br^- is assayed by ion chromatography using a Dionex® 1100 ion chromatograph equipped with an ASRS 300 4 mm conductivity detector. The

mobile phase is 8 mM Na₂CO₃/1 mM NaHCO₃ and the method is run isocratically at 0.7 mL min⁻¹ using an IonPac® AG14A 5 μm 3 × 30 mm guard column and an IonPac® AS14A 5 μm 3 × 150 mm analytical column (Lawrinenko et al. 2017). Lawrinenko et al. (2017) reported that pyrolysis temperature and the distribution of metal oxyhydroxides in biochar prepared by slow pyrolysis of biomass pre-treated with Al or Fe trichlorides strongly influenced biochar AEC. Biochar produced at 700 °C exhibits greater AEC than biochar prepared at 500 °C.

5 Surface Analyses

5.1 *Fourier-Transform Infrared Spectroscopy (FTIR)*

FTIR spectroscopy is a quick and cost-effective method to examine the surface of materials. The laboratory-based FTIR and Raman spectroscopy imaging effectively provides a deeper understanding of the chemical reactions occurring during biochar production, and the distribution of chemical phases on micron and millimeter scales (Chia et al. 2012). Multiple linear regression functions could explain the infrared absorption behavior as analyzed by FTIR spectra for specific regions of functional groups with coefficients of determination mostly from 60 to 90% (Janu et al. 2021). FTIR analyses can be performed using infrared spectroscopy for example the Thermo Scientific Nicolet iZ10 FT-IR spectrometer—the module of Thermo Scientific Nicolet iN10 MX microscope equipped with a Smart iTX accessory with a diamond plate (Wiercik et al. 2020) or DRIFTS (diffuse reflectance infrared Fourier transform spectroscopy; instrument: Bruker Tensor 37 with microtiter plate module Bruker HTS-XT) (Rodriguez et al. 2021). Each spectrum is usually an average of 32 or 64 scans in the 400–4000 cm⁻¹ wave-number range at the 4 cm⁻¹ spectral resolution (Janu et al. 2021).

Pyrolysis temperature impact the functional groups of biochar. Some workers (Sahoo et al. 2021) reported a decrease in the polar functional groups with an increase in pyrolysis temperature. Hydrophobic chars with very few functional groups were obtained at a higher pyrolysis temperature of 600 °C, due to more dehydration and deoxygenation reactions. They were characterized by a well-assembled layer of carbon. This agreed with the findings of another group of workers (Ahmad et al. 2014). This method could help to get a quick overview of the usability of different biochar for the immobilization of specific environmental contaminants or long-term carbon sequestration (Janu et al. 2021).

5.2 Scanning Electron Microscope (SEM)

A scanning electron microscope (SEM) is used to characterize the biochar morphology. SEM images give detailed descriptions regarding the microporous/mesoporous distributions and pore arrangement present in the biochar. The surface morphology before and after the adsorption process can be predicted using SEM (Yaashikaa et al. 2020). For SEM analyses, the samples are placed on supports with copper surfaces, followed by the application of a thin layer of gold (Veiga et al. 2021). The microscope used has a resolution of 3 nm and a zoom range of $10 \times 60,000$ (Munar-Florez et al. 2021). SEM pictures of biochar demonstrate changes in the surface morphology of the biochar particles due to pyrolysis. Additionally, the increasing temperature may bring about a huge improvement in the pore properties of biochar (Yaashikaa et al. 2020). However, intensified degree of carbonation of biochar at 700 °C leads to the destruction of the porous structure of biochar (Maljaee et al. 2021).

5.3 Specific Surface Area (BET)

In the process of pyrolysis, the pore structure is formed as there is the precipitation of volatile matter from the biomass. The process of carbonization makes a certain specific surface area and pore volume in biochar (Kong et al. 2021). The surface area of biochar can be examined using BET analysis. The study of the specific surface area is important because this property of biochar is mainly responsible for pollutant removal from soil and aqueous environment.

The higher temperatures of pyrolysis result in mass loss increase while providing biochar with a higher specific surface area (Howell et al. 2021). In general, the high carbonization temperature (450, 550, 650 °C) allows an enlarged specific surface area of produced biochar (Kong et al. 2021). On other hand, some workers (Ramola et al. 2020) found that the surface area of the biochar-mineral composite increases up to pyrolysis temperature of 500 °C, and then above 700 °C starts to decrease. It shows that optimum temperature is required for a high surface area of biochar. The reason for this can be the recondensation of volatilized organic compounds from the biochar-mineral composite on its surface that resulted in blocked pores and decreased surface area.

6 Molecular Analyses

Besides the positive effects of biochar, some negative effects “the dark side of the biochar” have also been reported (Bernardo et al. 2010; Gell et al. 2011; Rogovska et al. 2012; Quilliam et al. 2012; Loppinet-Serani et al. 2013; Oleszczuk et al. 2013;

Kloss et al. 2014; Buss and Mašek 2014; Białowiec et al. 2018). Contaminants within biochar may pose an environmental risk. Several studies have determined the total and bioavailable concentrations of heavy metals and polycyclic aromatic hydrocarbons (PAHs) in biochar prepared from various raw materials under various torrefaction and pyrolysis conditions (Spokas et al. 2011). It has been also confirmed that PAHs in biochar is suspected to have been responsible for acute toxicity to various organisms (Rogovska et al. 2012; Oleszczuk et al. 2013).

Biochar has the potential to introduce toxic chemicals into the soil that could damage soil functions. Three groups of potentially toxic substances, namely: metals and metalloids (such as, As, Cu, Pb, Ni, Zn, etc.); PAHs; dioxins, and other compounds, are the most likely agents to be present in biochar. Although environmental impacts attributable to metals, metalloids, PAHs, and dioxins associated with biochar are likely to be minimal (Hale et al. 2012; Freddo et al. 2012), special care is required to ensure the raw material, particularly biowastes, are not overly burdened with high concentrations of metals, metalloids, or chlorinated compounds (that may serve as dioxin precursors). Spokas et al. (2011), studied 77 different biochars produced from various raw materials in temperatures ranging from 200 to 800 °C. The analyses showed that biochar contained 140 different chemical compounds and 77 of these chemicals were common for each biochar.

Biochar prepared at lower pyrolytic temperatures (≤ 350 °C) produced VOCs consisting of short carbon chain aldehydes, furans, and ketones. Biochar prepared at elevated temperature (>350 °C) typically were dominated by aromatic compounds and longer carbon chain hydrocarbons. Similar conclusions came from (Wang et al. 2017) as the minimum concentration of PAH was observed in slow pyrolysis and longer retention (inside reactor) time. All the identified compounds in biochar prepared from RDF are organized into five groups (Białowiec et al. 2019). These are: (i) alkyl derivatives of benzene or phenols (32 compounds), (ii) alkyl derivatives of two-ring aromatic hydrocarbon (16 compounds), (iii) derivatives of heterocyclic amines (7 compounds), (iv) compounds that are generally considered as lower risk (e.g., present naturally in food) (22 compounds), (v) compounds that belong to other groups or with unknown structures (7 compounds).

The content of heavy metals including As, Cd, Cr, Co, Cu, Zn, Pb, Mo, and Ni can be easily analyzed with the application of ICP-AES or MP-AES after microwave-assisted aqua regia digestion. Organic pollutants content in biochar may be determined with the application of the following methods and protocols:

- (i) Qualitative and quantitative analyses of PAH is determined using the approach described in (Hilber et al. 2012; Wang et al. 2017; Geiss et al. 2018). The sample of biochar is extracted with a nonpolar solvent (hexane or dichloromethane), and if necessary concentrated on MIP-SPE cartridges. Samples may be analyzed in liquid injection techniques on GC-MS. Quantification is based on available standards covering Acenaphthylene, Anthracene, Benz[a]anthracene, Benzo[b]fluoranthene, Benzo[k]fluoranthene, Benzo[ghi]perylene, Benzo[a]pyrene, Chrysene,

- Dibenz[a,h]anthracene, FluoreneIndeno[1,2,3-cd]pyrene, Phenanthrene, Pyrene.
- (ii) Dioxins/Furans (PCDD/Fs) are analyzed according to US EPA 8290 (2007).
 - (iii) The NMR analyses of biochar are performed according to (Mao et al. 2013; Hmid et al. 2014) to characterize wide varieties of leachable compounds.
 - (iv) PAH and PCA (polychlorinated aromatic) are also analyzed using the LC–MS approach. Biochar sample is extracted with nonpolar solvent (hexane or dichloromethane), and if necessary concentrated on MIP-SPE or equivalent cartridges. A sample is submitted to LC–MS with MRM (multiple reaction monitoring) mode. Quantification is based on standards. Equipment parameters may be set according to (Bucheli et al. 2015).
 - (v) Measurements of VOCs may be done according to (Białowiec et al. 2018) headspace (HS) solid-phase microextraction (SPME) methodology for gas extraction and gas chromatography coupled with mass spectrometry (GC–MS) for analyses.

The application of the presented protocols allows for the determination of potentially harmful effects of biochar on the environment and humans. Moreover, humans can be exposed to biochar-associated (toxic) heavy metals, PAHs, and VOCs either directly through inhalation of particles or indirectly through the ingestion of fruits/vegetables grown in biochar-amended soil. Such exposure can pose a significant threat to human health due to the toxic, mutagenic, and carcinogenic effects of VOCs and PAHs. People involved in the handling, storage, and application of VOC-rich biochar could be exposed to VOCs that can pose a threat to health. Therefore, it is important to monitor these threats.

7 Limitations of Characterization of Engineered Biochar

The term “biochar” as a research topic, started to grow in 2009 when only 41 documents on this topic were available on the Web of Science. Since then, the research about biochar has grown exponentially reaching well over 5000 publications in 2021. In the early years of biochar research, awareness and understanding of the properties of biochar were low and it resulted in applying methods originally established for soils, fertilizers, and composts instead of developing analytical methods for biochar. As a result, biochar characterization methods vary and are not standardized (Igalavithana et al. 2017).

Some workers (Bachmann et al. 2016) considered the challenges associated with biochar analyses standardization. In their study, 3 biochar were prepared and homogenized, and subsequently sent to 22 independent laboratories in 12 countries for the determination of their properties. Roughly, 38 physical and chemical parameters were analyzed by each laboratory. The laboratories applied their discretion to choose the preferred method(s) to adopt for biochar characterization since their objective involved comparing the estimated reliability of the obtained analyzed results.

These workers demonstrated a good or at least acceptable degree of intralaboratory repeatability, despite the variations in interlaboratory results (Bachmann et al. 2016).

8 Conclusions and Future Prospects

Biochar properties can be measured by a wide range of analyses from basic physical to advance molecular analysis and each analysis can be conducted in several ways. Each type of analysis has a different purpose and meaning. However, due to the wide variability of biochar and their numerous application, specific analyses should be considered regarding the final application. Some recommendations about biochar analyses performance have been put forward (Nartey and Zhao 2014; Bachmann et al. 2016; Igalavithana et al. 2017). However, considering the vast biochar types, their applications, and various laboratory equipment available for researchers, the development of an international standard for use in the near future by the majority seems unlikely. It is more probable that the current existing/sophisticated analytical methods will continue to undergo modifications, which would enable the adoption/creation of enhanced/novel descriptions of biochar properties to emerge.

References

- Ahmad M, Lee SS, Dou X et al (2012) Effects of pyrolysis temperature on soybean stover- and peanut shell-derived biochar properties and TCE adsorption in water. *Biores Technol* 118:536–544. <https://doi.org/10.1016/j.biortech.2012.05.042>
- Ahmad M, Rajapaksha AU, Lim JE et al (2014) Biochar as a sorbent for contaminant management in soil and water: a review. *Chemosphere* 99:19–33. <https://doi.org/10.1016/j.chemosphere.2013.10.071>
- Al-Wabel MI, Al-Omran A, El-Naggar AH et al (2013) Pyrolysis temperature induced changes in characteristics and chemical composition of biochar produced from conocarpus wastes. *Biores Technol* 131:374–379. <https://doi.org/10.1016/j.biortech.2012.12.165>
- Ambaye TG, Vaccari M, van Hullebusch ED et al (2021) Mechanisms and adsorption capacities of biochar for the removal of organic and inorganic pollutants from industrial wastewater. *Int J Environ Sci Technol* 18:3273–3294. <https://doi.org/10.1007/s13762-020-03060-w>
- Anderson J Mercury Porosimetry. <https://www.mri.psu.edu/materials-characterization-lab/characterization-techniques/mercury-porosimetry>. Accessed 22 Jun 2021
- Bachmann HJ, Bucheli TD, Dieguez-Alonso A et al (2016) Toward the standardization of biochar analysis: the COST action TD1107 interlaboratory comparison. *J Agric Food Chem* 64:513–527. <https://doi.org/10.1021/acs.jafc.5b05055>
- Bartoli M, Giorcelli M, Jagdale P et al (2020) A review of non-soil biochar applications. *Materials* 13:261. <https://doi.org/10.3390/ma13020261>
- Basu P (2018) Biomass combustion and cofiring. In: *Biomass gasification, pyrolysis and torrefaction: practical design and theory*. Elsevier, pp 393–413
- Batista EMCC, Shultz J, Matos TTS et al (2018) Effect of surface and porosity of biochar on water holding capacity aiming indirectly at preservation of the Amazon biome. *Sci Rep* 8. <https://doi.org/10.1038/s41598-018-28794-z>

- Bernardo M, Lapa N, Gonçalves M et al (2010) Toxicity of char residues produced in the co-pyrolysis of different wastes. *Waste Manage* 30:628–635. <https://doi.org/10.1016/j.wasman.2009.10.015>
- Białowiec A, Micuda M, Szumny A et al (2018) Quantification of VOC emissions from carbonized refuse-derived fuel using solid-phase microextraction and gas chromatography-mass spectrometry. *Molecules* 23. <https://doi.org/10.3390/molecules23123208>
- Białowiec A, Micuda M, Szumny A et al (2019) The proof-of-the-concept of application of pelletization for mitigation of volatile organic compounds emissions from carbonized refuse-derived fuel. *Materials* 12. <https://doi.org/10.3390/ma12101692>
- Bian R, Li L, Shi W et al (2018) Pyrolysis of contaminated wheat straw to stabilize toxic metals in biochar but recycle the extract for agricultural use. *Biomass Bioenerg* 118:32–39. <https://doi.org/10.1016/j.biombioe.2018.08.003>
- Brewer CE, Chuang VJ, Masiello CA et al (2014) New approaches to measuring biochar density and porosity. *Biomass Bioenerg* 66:176–185. <https://doi.org/10.1016/j.biombioe.2014.03.059>
- Bucheli TD, Hilber I, Schmidt H-P (2015) Polycyclic aromatic hydrocarbons and polychlorinated aromatic compounds in biochar. In: *Biochar for environmental management*. pp 595–624
- Buss W, Mašek O (2014) Mobile organic compounds in biochar—a potential source of contamination—phytotoxic effects on cress seed (*Lepidiumsativum*) germination. *J Environ Manage* 137:111–119. <https://doi.org/10.1016/j.jenvman.2014.01.045>
- Caillat S, Vakkilainen E (2013) Large-scale biomass combustion plants: an overview. In: *Biomass combustion science, technology and engineering*. Elsevier, pp 189–224
- Carrier M, Loppinet-Serani A, Denux D et al (2011) Thermogravimetric analysis as a new method to determine the lignocellulosic composition of biomass. *Biomass Bioenerg* 35:298–307. <https://doi.org/10.1016/j.biombioe.2010.08.067>
- Chen B, Koziel JA, Białowiec A et al (2021a) Mitigation of acute ammonia emissions with biochar during swine manure agitation before pump-out: proof-of-the-concept. *Front Environ Sci* 9. <https://doi.org/10.3389/fenvs.2021a.613614>
- Cheng CH, Lehmann J, Engelhard MH (2008) Natural oxidation of black carbon in soils: changes in molecular form and surface charge along a climosequence. *Geochim Cosmochim Acta* 72:1598–1610. <https://doi.org/10.1016/j.gca.2008.01.010>
- Chia CH, Gong B, Joseph SD et al (2012) Imaging of mineral-enriched biochar by FTIR, Raman and SEM-EDX. *Vib Spectrosc* 62:248–257. <https://doi.org/10.1016/j.vibspec.2012.06.006>
- Das KC, Singh K, Adolphson R et al (2010) Steam pyrolysis and catalytic steam reforming of biomass for hydrogen and biochar production. *Appl Eng Agric* 26:137–146
- Freddo A, Cai C, Reid BJ (2012) Environmental contextualisation of potential toxic elements and polycyclic aromatic hydrocarbons in biochar. *Environ Pollut* 171:18–24. <https://doi.org/10.1016/j.envpol.2012.07.009>
- Gabhi RS, Kirk DW, Jia CQ (2017) Preliminary investigation of electrical conductivity of monolithic biochar. *Carbon* 116:435–442. <https://doi.org/10.1016/j.carbon.2017.01.069>
- Geiss O, Senaldi C, Bianchi I et al (2018) A fast and selective method for the determination of 8 carcinogenic polycyclic aromatic hydrocarbons in rubber and plastic materials. *J Chromatogr A* 1566:13–22. <https://doi.org/10.1016/j.chroma.2018.06.047>
- Gell K, van Groenigen JW, Cayuela ML (2011) Residues of bioenergy production chains as soil amendments: immediate and temporal phytotoxicity. *J Hazard Mater* 186:2017–2025. <https://doi.org/10.1016/j.jhazmat.2010.12.105>
- Hale SE, Elmquist M, Brändli R et al (2012) Activated carbon amendment to sequester PAHs in contaminated soil: a lysimeter field trial. *Chemosphere* 87:177–184. <https://doi.org/10.1016/j.chemosphere.2011.12.015>
- Hilber I, Blum F, Leifeld J et al (2012) Quantitative determination of PAHs in biochar: a prerequisite to ensure its quality and safe application. *J Agric Food Chem* 60:3042–3050. <https://doi.org/10.1021/jf205278v>
- Hmid A, Mondelli D, Fiore S et al (2014) Production and characterization of biochar from three-phase olive mill waste through slow pyrolysis. *Biomass Bioenerg* 71:330–339. <https://doi.org/10.1016/j.biombioe.2014.09.024>

- Hosokai S, Matsuoka K, Kuramoto K, Suzuki Y (2016) Modification of Dulong's formula to estimate heating value of gas, liquid and solid fuels. *Fuel Process Technol* 152:399–405. <https://doi.org/10.1016/j.fuproc.2016.06.040>
- Howell N, Pimentel A, Bhattacharia S (2021) Material properties and environmental potential of developing world-derived biochar made from common crop residues. *Environ Chall* 4:100137. <https://doi.org/10.1016/j.envc.2021.100137>
- Huff MD, Marshall S, Saeed HA, Lee JW (2018) Surface oxygenation of biochar through ozonization for dramatically enhancing cation exchange capacity. *Bioresour Bioprocess* 5. <https://doi.org/10.1186/s40643-018-0205-9>
- Igalavithana AD, Mandal S, Niazi NK et al (2017) Advances and future directions of biochar characterization methods and applications. *Crit Rev Environ Sci Technol* 47:2275–2330. <https://doi.org/10.1080/10643389.2017.1421844>
- Jafri N, Wong WY, Doshi V et al (2018) A review on production and characterization of biochars for application in direct carbon fuel cells. *Process Saf Environ Prot* 118:152–166. <https://doi.org/10.1016/j.psep.2018.06.036>
- Janu R, Mrlik V, Ribitsch D et al (2021) Biochar surface functional groups as affected by biomass feedstock, biochar composition and pyrolysis temperature. *Carbon Resour Convers* 4:36–46. <https://doi.org/10.1016/j.crcon.2021.01.003>
- Jeon J, Kim HI, Park JH et al (2021) Evaluation of thermal properties and acetaldehyde adsorption performance of sustainable composites using waste wood and biochar. *Environ Res* 196. <https://doi.org/10.1016/j.envres.2021.110910>
- Kameyama K, Miyamoto T, Iwata Y (2019) The preliminary study of water-retention related properties of biochar produced from various feedstock at different pyrolysis temperatures. *Materials* 12. <https://doi.org/10.3390/ma12111732>
- Kelly Orhorhoro E, Okechukwu E, Ejuvwedia Sadjere G (2017) Experimental determination of effect of total solid (TS) and volatile solid (VS) on biogas yield. *Am J Mod Energy* 3:131. <https://doi.org/10.11648/j.ajme.20170306.13>
- Kim G-M, Jeong J-W, Jeong J-S et al (2019) Empirical formula to predict the NO_x emissions from coal power plant using lab-scale and real-scale operating data. *Appl Sci* 9:2914. <https://doi.org/10.3390/app9142914>
- Kinney TJ, Masiello CA, Dugan B et al (2012) Hydrologic properties of biochars produced at different temperatures. *Biomass Bioenerg* 41:34–43. <https://doi.org/10.1016/j.biombioe.2012.01.033>
- Kloss S, Zehetner F, Wimmer B et al (2014) Biochar application to temperate soils: effects on soil fertility and crop growth under greenhouse conditions. *J Plant Nutr Soil Sci* 177:3–15. <https://doi.org/10.1002/jpln.201200282>
- Kong W, Zhang M, Liu Y et al (2021) Physico-chemical characteristics and the adsorption of ammonium of biochar pyrolyzed from distilled spirit lees, tobacco fine and Chinese medicine residues. *J Anal Appl Pyrol* 156. <https://doi.org/10.1016/j.jaap.2021.105148>
- Lachman J, Baláš M, Lisý M et al (2021) An overview of slagging and fouling indicators and their applicability to biomass fuels. *Fuel Process Technol* 217:106804. <https://doi.org/10.1016/j.fuproc.2021.106804>
- Lawrinenko M, Jing D, Banik C, Laird DA (2017) Aluminum and iron biomass pretreatment impacts on biochar anion exchange capacity. *Carbon* 118:422–430. <https://doi.org/10.1016/j.carbon.2017.03.056>
- Lawrinenko M, Laird DA (2015) Anion exchange capacity of biochar. *Green Chem* 17:4628–4636. <https://doi.org/10.1039/c5gc00828j>
- Lee JW, Buchanan AC, Evans BR, Kidder M (2013) Oxygenation of biochar for enhanced cation exchange capacity. *Advanced biofuels and bioproducts*. Springer, New York, pp 35–45
- Lee M, Koziel JA, Murphy W et al (2021) Mitigation of odor and gaseous emissions from swine barn with UV-A and UV-C photocatalysis. *Atmosphere* 12. <https://doi.org/10.3390/atmos12050585>

- Li S, Chen G (2018) Thermogravimetric, thermochemical, and infrared spectral characterization of feedstocks and biochar derived at different pyrolysis temperatures. *Waste Manage* 78:198–207. <https://doi.org/10.1016/j.wasman.2018.05.048>
- Loppinet-Serani A, Reverte C, Cansell F, Aymonier C (2013) Supercritical water biomass gasification process as a successful solution to valorize wine distillery wastewaters. *ACS Sustain Chem Eng* 1:110–117. <https://doi.org/10.1021/sc300058f>
- Malinowski M, Wolny-Koładka K, Vaverková MD (2019) Effect of biochar addition on the OFMSW composting process under real conditions. *Waste Manage* 84:364–372. <https://doi.org/10.1016/j.wasman.2018.12.011>
- Maljaee H, Madadi R, Paiva H et al (2021) Incorporation of biochar in cementitious materials: a roadmap of biochar selection. *Constr Build Mater* 283:122757. <https://doi.org/10.1016/j.conbuildmat.2021.122757>
- Mao J, Cao X, Chen N (2013) Characterization of biochars using advanced solid-state ¹³C nuclear magnetic resonance spectroscopy. *Advanced biofuels and bioproducts*. Springer, New York, pp 47–55
- Masís-Meléndez F, Segura-Chavarría D, García-González CA et al (2020) Variability of physical and chemical properties of TLUD stove derived biochars. *Appl Sci* 10. <https://doi.org/10.3390/app10020507>
- Mayer ZA, Eltom Y, Stennett D et al (2014) Characterization of engineered biochar for soil management. *Environ Prog Sustainable Energy* 33:490–496. <https://doi.org/10.1002/ep.11788>
- Morales VL, Pérez-Reche FJ, Hapca SM et al (2015) Reverse engineering of biochar. *Biores Technol* 183:163–174. <https://doi.org/10.1016/j.biortech.2015.02.043>
- Munar-Florez DA, Varón-Cardenas DA, Ramírez-Contreras NE, García-Núñez JA (2021) Adsorption of ammonium and phosphates by biochar produced from oil palm shells: effects of production conditions. *Results Chem* 3. <https://doi.org/10.1016/j.rechem.2021.100119>
- Nartey OD, Zhao B (2014) Biochar preparation, characterization, and adsorptive capacity and its effect on bioavailability of contaminants: an overview. *Adv Mater Sci Eng* 2014:1–12. <https://doi.org/10.1155/2014/715398>
- Narzari R, Bordoloi N, Chutia RS et al (2015) Biochar: an overview on its production, properties and potential benefits. In: Choudhury H (ed) *Biology, biotechnology and sustainable development*. Research India Publications, Delhi
- Nunes LJR, de Oliveira Matias JC, da Silva Catalão JP (2018) Introduction. In: *Torrefaction of biomass for energy applications*. Elsevier, pp 1–43
- Oleszczuk P, Joško I, Kuśmierz M (2013) Biochar properties regarding to contaminants content and ecotoxicological assessment. *J Hazard Mater* 260:375–382. <https://doi.org/10.1016/j.jhazmat.2013.05.044>
- Oliveira FR, Patel AK, Jaisi DP et al (2017) Environmental application of biochar: current status and perspectives. *Biores Technol* 246:110–122. <https://doi.org/10.1016/j.biortech.2017.08.122>
- Paar A. Pore size measurement techniques. <https://wiki.anton-paar.com/en/pore-size-measurement/>. Accessed 13 Jun 2021
- Plötze M, Niemi P (2011) Porosity and pore size distribution of different wood types as determined by mercury intrusion porosimetry. *Eur J Wood Wood Prod* 69:649–657. <https://doi.org/10.1007/s00107-010-0504-0>
- Pudasainee D, Kurian V, Gupta R (2020) Coal. In: *Future energy*. Elsevier, pp 21–48
- Quilliam RS, Marsden KA, Gertler C et al (2012) Nutrient dynamics, microbial growth and weed emergence in biochar amended soil are influenced by time since application and reapplication rate. *Agr Ecosyst Environ* 158:192–199. <https://doi.org/10.1016/j.agee.2012.06.011>
- Ramola S, Belwal T, Li CJ et al (2020) Improved lead removal from aqueous solution using novel porous bentonite- and calcite-biochar composite. *Sci Total Environ* 709:136171. <https://doi.org/10.1016/j.scitotenv.2019.136171>
- Ramola S, Mishra T, Rana G, Srivastava RK (2014) Characterization and pollutant removal efficiency of biochar derived from baggase, bamboo and tyre. *Environ Monit Assess* 186:9023–9039. <https://doi.org/10.1007/s10661-014-4062-5>

- Repellin V, Govin A, Rolland M, Guyonnet R (2010) Energy requirement for fine grinding of torrefied wood. *Biomass Bioenerg* 34:923–930. <https://doi.org/10.1016/j.biombioe.2010.01.039>
- Rippy JFM, Nelson PV (2007) Cation exchange capacity and base saturation variation among Alberta, Canada, Moss Peats. *Hort Sci* 42:349–352
- Rizwan M, Ali S, Qayyum MF et al (2016) Mechanisms of biochar-mediated alleviation of toxicity of trace elements in plants: a critical review. *Environ Sci Pollut Res* 23:2230–2248. <https://doi.org/10.1007/s11356-015-5697-7>
- Rodriguez JA, Lustosa Filho JF, Melo LCA et al (2021) Co-pyrolysis of agricultural and industrial wastes changes the composition and stability of biochars and can improve their agricultural and environmental benefits. *J Anal Appl Pyrol* 155. <https://doi.org/10.1016/j.jaap.2021.105036>
- Rogovska N, Laird D, Cruse RM et al (2012) Germination tests for assessing biochar quality. *J Environ Qual* 41:1014–1022. <https://doi.org/10.2134/jeq2011.0103>
- Safdari M-S, Rahmati M, Amini E et al (2018) Characterization of pyrolysis products from fast pyrolysis of live and dead vegetation native to the Southern United States. *Fuel* 229:151–166. <https://doi.org/10.1016/j.fuel.2018.04.166>
- Sahoo SS, Vijay VK, Chandra R, Kumar H (2021) Production and characterization of biochar produced from slow pyrolysis of pigeon pea stalk and bamboo. *Clean Eng Technol* 3:100101. <https://doi.org/10.1016/j.clet.2021.100101>
- Santín C, Doerr SH, Merino A et al (2017) Carbon sequestration potential and physicochemical properties differ between wildfire charcoals and slow-pyrolysis biochars. *Sci Rep* 7:11233. <https://doi.org/10.1038/s41598-017-10455-2>
- Shao L, Li S, Cai J et al (2019) Ability of biochar to facilitate anaerobic digestion is restricted to stressed surroundings. *J Clean Prod* 238. <https://doi.org/10.1016/j.jclepro.2019.117959>
- Spokas KA, Novak JM, Stewart CE et al (2011) Qualitative analysis of volatile organic compounds on biochar. *Chemosphere* 85:869–882. <https://doi.org/10.1016/j.chemosphere.2011.06.108>
- Stegenta-Dąbrowska S, Randerson PF, Christofides SR, Białowiec A (2020) Carbon monoxide formation during aerobic biostabilization of the organic fraction of municipal solid waste: the influence of technical parameters in a full-scale treatment system. *Energies* 13:5624. <https://doi.org/10.3390/en13215624>
- Suárez-Ruiz I, Ward CR (2008) Basic factors controlling coal quality and technological behavior of coal. In: *Applied coal petrology*. Elsevier, pp 19–59
- Świechowski K, Liszewski M, Bąbalewski P et al (2019) Fuel properties of torrefied biomass from pruning of Oxytree. *Data* 4:55. <https://doi.org/10.3390/data4020055>
- Świechowski K, Stępień P, Syguła E et al (2021) Lab-scale study of temperature and duration effects on carbonized solid fuels properties produced from municipal solid waste components. *Materials* 14:1191. <https://doi.org/10.3390/ma14051191>
- Świechowski K, Syguła E, Koziel JA et al (2020) Low-temperature pyrolysis of municipal solid waste components and refuse-derived fuel—process efficiency and fuel properties of carbonized solid fuel. *Data* 5:48. <https://doi.org/10.3390/data5020048>
- Thompson M (2008) CHNS elemental analysers
- Thrush PW (1968) Definition of coal fuel ratio. In: Bureau of mines, Department of the Interior. https://www.mindat.org/glossary/coal_fuel_ratio. Accessed 29 May 2021
- Tomczyk A, Sokołowska Z, Boguta P (2020) Biochar physicochemical properties: pyrolysis temperature and feedstock kind effects. *Rev Environ Sci Biotechnol* 19:191–215. <https://doi.org/10.1007/s11157-020-09523-3>
- Torquato LDM, Crnkovic PM, Ribeiro CA, Crespi MS (2017) New approach for proximate analysis by thermogravimetry using CO₂ atmosphere: validation and application to different biomasses. *J Therm Anal Calorim* 128. <https://doi.org/10.1007/s10973-016-5882-z>
- Trakal L, Veselská V, Šafařík I et al (2016) Lead and cadmium sorption mechanisms on magnetically modified biochars. *Biores Technol* 203:318–324. <https://doi.org/10.1016/j.biortech.2015.12.056>
- da Silva Veiga PA, Cerqueira MH, Gonçalves MG et al (2021) Upgrading from batch to continuous flow process for the pyrolysis of sugarcane bagasse: Structural characterization of the biochars produced. *J Environ Manag* 285. <https://doi.org/10.1016/j.jenvman.2021.112145>

- Wade JB, Martin GP, Long DF (2015) An assessment of powder pycnometry as a means of determining granule porosity. *Pharm Dev Technol* 20:257–265. <https://doi.org/10.3109/10837450.2013.860550>
- Wang C, Wang Y, Herath HMSK (2017) Polycyclic aromatic hydrocarbons (PAHs) in biochar—their formation, occurrence and analysis: a review. *Org Geochem* 114:1–11. <https://doi.org/10.1016/j.orggeochem.2017.09.001>
- Wang P, Howard BH (2018) Impact of thermal pretreatment temperatures on woody biomass chemical composition, physical properties and microstructure. *Energies* 11:25. <https://doi.org/10.3390/en11010025>
- Wani I, Ramola S, Garg A, Kushvaha V (2021) Critical review of biochar applications in geo-engineering infrastructure: moving beyond agricultural and environmental perspectives. *Biomass Convers Biorefin*. <https://doi.org/10.1007/s13399-021-01346-8>
- Webb PA (2001) Volume and density determinations for particle technologists. Micromeritics Instrument Corp
- Weber K, Quicker P (2018) Properties of biochar. *Fuel* 217:240–261. <https://doi.org/10.1016/j.fuel.2017.12.054>
- Werner K, Pommer L, Broström M (2014) Thermal decomposition of hemicelluloses. *J Anal Appl Pyrol* 110:130–137. <https://doi.org/10.1016/j.jaap.2014.08.013>
- Wiercik P, Frączek B, Chrobot P (2020) Fouling of anion exchanger by image and FTIR analyses. *J Environ Chem Eng* 8. <https://doi.org/10.1016/j.jece.2020.103761>
- Yaashikaa PR, Kumar PS, Varjani S, Saravanan A (2020) A critical review on the biochar production techniques, characterization, stability and applications for circular bioeconomy. *Biotechnol Rep* 28
- Yang X, Wang H, Strong PJ et al (2017) Thermal properties of biochars derived from waste biomass generated by agricultural and forestry sectors. *Energies* 10. <https://doi.org/10.3390/en10040469>
- Zhang C, Ho S-H, Chen W-H et al (2018) Torrefaction performance and energy usage of biomass wastes and their correlations with torrefaction severity index. *Appl Energy* 220:598–604. <https://doi.org/10.1016/j.apenergy.2018.03.129>
- Zhao Z, Cao Y, Li S, Zhang Y (2021) Effects of biowaste-derived biochar on the electron transport efficiency during anaerobic acid orange 7 removal. *Bioresour Technol* 320. <https://doi.org/10.1016/j.biortech.2020.124295>